

# ChemComm

Accepted Manuscript



This article can be cited before page numbers have been issued, to do this please use: L. Qin, B. Wang, Y. Zhang, L. Chen and G. Gao, *Chem. Commun.*, 2017, DOI: 10.1039/C6CC10158E.



This is an Accepted Manuscript, which has been through the Royal Society of Chemistry peer review process and has been accepted for publication.

Accepted Manuscripts are published online shortly after acceptance, before technical editing, formatting and proof reading. Using this free service, authors can make their results available to the community, in citable form, before we publish the edited article. We will replace this Accepted Manuscript with the edited and formatted Advance Article as soon as it is available.

You can find more information about Accepted Manuscripts in the [author guidelines](#).

Please note that technical editing may introduce minor changes to the text and/or graphics, which may alter content. The journal's standard [Terms & Conditions](#) and the ethical guidelines, outlined in our [author and reviewer resource centre](#), still apply. In no event shall the Royal Society of Chemistry be held responsible for any errors or omissions in this Accepted Manuscript or any consequences arising from the use of any information it contains.



ChemComm

## COMMUNICATION

# Anion Exchange: A Novel Way for Preparing Hierarchical Porous Structure of Poly(ionic liquid)s. †

Received 00th January 20xx,  
Accepted 00th January 20xx

Li Qin, Binshen Wang, Yongya Zhang, Li Chen and Guohua Gao\*

DOI: 10.1039/x0xx00000x

www.rsc.org/

**Hierarchical porous poly(ionic liquid)s (PILs) with high specific surface area were synthesized *via* anion exchange firstly. The bulky salicylate and its dimers/clusters of PILs exchanged by other smaller anions increased specific surface area and fabricated hierarchical porous structure. The high specific surface area and hierarchical porous structure prompted a high degree of exposure of the active sites and made the heterogeneous PIL catalysts contact with substrates sufficiently, enhancing their catalytic activity.**

Poly(ionic liquid)s (PILs), which possess an ionic liquid (IL) moiety in the repeating unit of the polymer chains, refer to a subclass of polyelectrolytes. Combining the intrinsic polymeric nature with specific properties stemming from ionic liquids (ILs),<sup>1</sup> PILs have been widely applied as promising materials in the field of catalysts,<sup>2</sup> polymer electrolytes,<sup>3</sup> carbon materials,<sup>4</sup> thermoresponsive materials,<sup>5</sup> separation and adsorption materials.<sup>6</sup> In order to increase the degree of exposure of the active sites in PILs and accelerate the interfacial mass and energy exchange, porous PILs have received increasing attention in catalysis.<sup>7-12</sup>

Many synthetic methods of porous PILs, which are aimed at increasing the specific surface area and fabricating pore structure of PILs, have been reported. These methods can be roughly classified into the following strategies: hard template, soft template, electrostatic complexation, solvothermal/ionothermal method and post-modification. Hard-templating method employs acid/base to etch the additive inorganic components (usually silica), which fill the interstitial voids of porous PILs, and forms an inverse opal and well-ordered macro-mesoporous structure.<sup>7,13</sup> Soft templating method utilizes the solvent extraction to remove the organic tri-block polymer template (P123) after polymerization of IL

monomers, which generates hierarchical meso-macroporous structure.<sup>8</sup> Electrostatic complexation approach exploits electrostatic complexation between cationic PILs and carboxylate anions in ammonia-containing solvent, triggers the in situ interpolyelectrolyte complexation and forms a three dimension net structure.<sup>11,14</sup> Solvothermal/ionothermal method relies on the free radical self-polymerization of monomeric ILs by using nonaqueous organic solvents or another conventional ILs as the solvents, respectively.<sup>9,15</sup> Post-modification method is *via* quaternization of the nitrogen atom per monomeric unit of non-ionic porous co-polymers such as divinylbenzene and vinylimidazole to introduce the ionic liquid functionality in the polymeric matrix.<sup>10,12,16</sup> Despite the significant advances of the synthesis of porous PILs in the past few years, the methods of fabricating porous PILs are still limited.

Anions occupy the interstitial voids in the process of polymerization of IL monomers. Thus theoretically, the bulky anions of PILs exchanged by smaller ones can release the occupied space and form porous structure. To the best of our knowledge, fabricating porous PILs *via* anion exchange has not been reported yet. Herein we describe a novel methodology for synthesis of porous PILs by anion exchange (Fig. 1). The salicylate was chosen as primary anion as it can form dimers/clusters through hydrogen bond between hydroxyl and carboxyl to generate different size of anions.<sup>17</sup> Thus, by

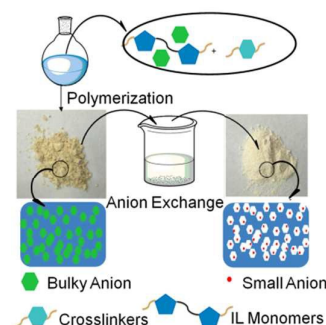


**Fig.1** Schematic illustration of synthesis of porous poly(ionic liquid)s by anion exchange.

\*Shanghai Key Laboratory of Green Chemistry and Chemical Processes, School of Chemistry and Molecular Engineering, East China Normal University, North Zhongshan Road 3663, Shanghai 200062, China, Fax: (+)86-21-62233323, e-mail: [ghgao@chem.ecnu.edu.cn](mailto:ghgao@chem.ecnu.edu.cn)

†Electronic Supplementary Information (ESI) available: [details of any supplementary information available should be included here]. See DOI:10.1039/x0xx00000x

Scheme 1 Synthetic routes of poly(ionic liquid)s.

exchanging salicylate or its dimers/clusters to other small anions, the obtained PILs may exhibit high specific surface area and hierarchical porous structure.

The typical procedure for preparation of porous PILs is as following: 1,4-Butanediyl-3,3'-bis-1-vinylimidazolium disalicylate (BVImSal, 0.04 mol, 20.74 g) and divinylbenzene (DVB, 0.08 mol, 10.41 g) were copolymerized using 2,2'-azobisisobutyronitrile (AIBN, 5 wt%, 1.64 g) as an initiator in methanol at reflux for 24 h. Poly(bisvinylimidazolium-base disalicylate) (PBVImSal) was obtained in a yellow powder. The anion exchange of PBVImSal was carried out by stirring in NaCl, NaBr, NaOAc saturated aqueous solutions respectively, at room temperature several times until the salicylate was exchanged completely (Scheme 1). The obtained porous PILs with different anions were denoted as AE-PIL-X, where AE represented anion exchange and X represented Cl<sup>-</sup>, Br<sup>-</sup>, OAc<sup>-</sup>, respectively. In comparison, the nonporous PILs with different anions (Cl<sup>-</sup>, Br<sup>-</sup> and OAc<sup>-</sup>) were directly synthesized by the copolymerization of corresponding 1,4-butanediyl-3,3'-bis-1-vinylimidazolium monomers (Detail synthesis and characterizations of ILs were supplied in ESI, Fig. S1 and S2, ESI<sup>†</sup>) with DVB under identical conditions (denoted as DS-PIL-X, where DS represented direct synthesis and X represented Cl<sup>-</sup>, Br<sup>-</sup>, OAc<sup>-</sup>, respectively).

The as synthesized PILs were characterized by NMR spectra. <sup>13</sup>C MAS NMR spectra of porous PILs and the <sup>13</sup>C NMR spectrum of BVImSal were presented in Fig. 2. Fully polymerization of carbon-carbon double bond of N-vinyl was confirmed by the disappearance of peak at 108 ppm (Fig. 2a and 2b). When salicylate anions were exchanged by acetates, carbonyl carbon downfield shifted from 173 to 177 ppm and phenolic hydroxyl carbon peak at 163 ppm disappeared (Fig. 2c). When salicylate anions were exchanged by halides (Cl<sup>-</sup>, Br<sup>-</sup>), the peaks at 173 ppm and 163 ppm disappeared (Fig. 2d and 2e). These results suggested that the Sal<sup>-</sup> in PILs had been completely exchanged by other anions such as Cl<sup>-</sup>, Br<sup>-</sup> and OAc<sup>-</sup>.

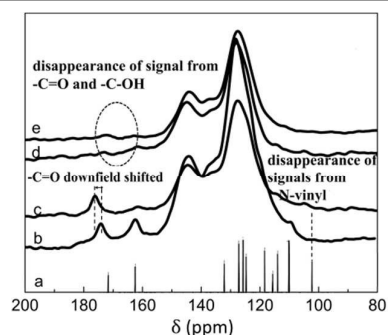


Fig. 2 <sup>13</sup>C NMR spectrum of a) BVImSal; <sup>13</sup>C MAS NMR spectra of b) PBVImSal; c) AE-PIL-OAc; d) AE-PIL-Cl and e) AE-PIL-Br.

The successful anion exchange also was supported by Fourier transform infrared spectroscopy (Fig. S3 and S4, ESI<sup>†</sup>). After the Sal<sup>-</sup> exchanged by OAc<sup>-</sup>, the C=O double bond stretching absorption peak at 1590 cm<sup>-1</sup> (salicylate) red shifted to 1578 cm<sup>-1</sup> (acetate). While the Sal<sup>-</sup> exchanged by halides (chloride, bromide), the C=O double bond absorption of salicylate stretching peak disappeared. Thermogravimetric (TG) analysis results showed that all PILs exhibited the weight loss at temperatures between 250–380 °C, and 410–500 °C, which are mainly attributed to the decomposition of the imidazoliums and DVB respectively (Fig. S5a and b, ESI<sup>†</sup>). The DSC analysis showed that all PILs did not have the glass transitions in the temperature from -50 to 200 °C (Fig. S6a, ESI<sup>†</sup>). The chemical composition of PILs was determined by CHN analysis (Table S1, ESI<sup>†</sup>) and the contents of imidazoliums of PILs according to nitrogen contents were 1.6–2.1 mmol/g of PILs.

The argon adsorption isotherms were measured at 77K to characterize the specific surface area, micropore area and pore size distribution. The specific surface area of PBVImSal was 15.1 m<sup>2</sup>/g (Table 1, entry 1). After anion exchange by NaCl, NaBr and NaOAc, all the specific surface area and micropore area of AE-PIL-X (X= Cl, Br and OAc) were increased significantly (Table 1, entries 2-4). The order of specific surface area was AE-PIL-Cl (227.5 m<sup>2</sup>/g) > AE-PIL-Br (180.6 m<sup>2</sup>/g) > AE-PIL-OAc (129.2 m<sup>2</sup>/g), which was opposite to the order of the anions size (Cl<sup>-</sup> < Br<sup>-</sup> < OAc<sup>-</sup>, Table S2, ESI<sup>†</sup>). Thereinto, the micropore areas are 50.7, 28.7 and 23.8 m<sup>2</sup>/g, respectively. These results indicated that after exchanged by other anions, the smaller anion (Cl<sup>-</sup>, Br<sup>-</sup> and OAc<sup>-</sup>) of porous PILs, the higher specific surface area was obtained. The argon sorption isotherms of AE-PIL-X exhibited a clear type-IV isotherm with hysteresis loop of type H3 at the P/P0 range from 0.3 to 0.99 (Fig. S7, ESI<sup>†</sup>). The pore size distribution curves (Fig. S8, ESI<sup>†</sup>) displayed that the AE-PIL-X were mainly composed of 0.6-1.0 nm micropores and 2-10 nm mesopores. The formations of micropores and mesopores were attributed to the exchange of salicylate and its dimers/clusters by the smaller anions, respectively. In comparison, those nonporous PILs (DS-PIL-X) showed low specific surface areas around 17.9-25.6 m<sup>2</sup>/g. The pore size distributions of the DS-PIL-X indicated no microporous structure and few 10-20 nm pores which might form by particle packing (Fig. S8, ESI<sup>†</sup>). The morphologies of AE-PIL-X and DS-PIL-X were visualized by SEM images (Fig. 3a-f). AE-PIL-X and DS-PIL-X were composed of around 50-200 nm round-shaped granules which were agglomerated by smaller particles. The result indicated that the particle size of porous PILs prepared by anion exchange was same to that of nonporous PILs synthesized directly. TEM images of the typical sample of AE-PIL-Cl provided a distinct mesoporous structure (Fig. 3g and h). All the above features showed a significant

**Table 1** The content of imidazolium and BET of PILs.

Entry	PILs	Im <sup>a</sup> (mmol/g)	S <sub>BET</sub> <sup>b</sup> (m <sup>2</sup> /g)	S <sub>micropor</sub> <sup>c</sup> (m <sup>2</sup> /g)	V <sup>d</sup> (cm <sup>3</sup> /g)
1	PBVImSal	1.9	15.1	4.4	0.03
2	AE-PIL-Cl	1.9	227.5	50.7	0.20
3	AE-PIL-Br	1.6	180.6	28.7	0.20
4	AE-PIL-OAc	1.6	129.2	23.8	0.14
5	DS-PIL-Cl	1.6	25.6	—	0.03
6	DS-PIL-Br	2.1	18.2	—	0.03
7	DS-PIL-OAc	1.7	17.9	1.9	0.02

<sup>a</sup>The mole amount of imidazolium was calculated by nitrogen content. <sup>b</sup>BET surface area was calculated by Ar isotherm. <sup>c</sup>t-plot micropore area. <sup>d</sup>Total pore volume.

effect of the anion exchange on increasing specific surface area and creating hierarchical porous structure.

Further study was focused on the relationship between specific surface area and catalytic activity of PILs. The cycloaddition reaction of CO<sub>2</sub> and epoxides using ILs or PILs as catalysts, which was extensively studied by other groups and our precious work<sup>11,18</sup> was chosen as a model reaction (Detailed studies on reaction conditions and proposed reaction course were supplied in Fig S9-11). When 1,2-epoxyhexane was used as substrate, AE-PIL-Cl displayed higher catalytic activity than that of DS-PIL-Cl. And AE-PIL-OAc and AE-PIL-Br also showed more superior catalytic activity than that of DS-PIL-OAc and DS-PIL-Br (Fig. S12, ESI<sup>†</sup>). Theoretically, the catalytic activity of bromide-based ILs is more efficient than that of chloride-base ILs in the reactions of epoxides and CO<sub>2</sub> because bromide promotes ring opening of epoxides owing to its good nucleophilicity and leaving ability.<sup>19</sup> It should be noted that AE-PIL-Cl gave slightly higher yields than those of AE-PIL-Br due to the higher specific surface area (227.5 m<sup>2</sup>/g > 180.6 m<sup>2</sup>/g) (Fig. S13, ESI<sup>†</sup>). When propylene oxide, epichlorohydrin, 1,2-epoxyoctane, 1,2-epoxydodecane and styrene oxide were used as reaction substrates, the superior catalytic activity of AE-PIL-Cl was also observed comparing with DS-PIL-Cl (Fig. 4). The differences of activity of AE-PIL-Cl and DS-PIL-Cl were in order of propylene oxide (6%) < epichlorohydrin (8%) < 1,2-epoxyhexane (19%) < 1,2-epoxyoctane (21%), 1,2-epoxydodecane (21%), which is consistent with the chain length of the epoxides. The relatively greater difference of yields (25%) between AE-PIL-Cl and DS-PIL-Cl was found in the

reaction of styrene oxide and CO<sub>2</sub> which may be attributed to the larger width of the epoxide (Table S3, ESI<sup>†</sup>). The comparison of the yields for all products clearly revealed that bulky substrate was more difficult to access the active sites of nonporous PILs. Given similar active sites in both AE-PIL-X and DS-PIL-X, the increase of catalytic activity can be ascribed to the increasing specific surface area and hierarchical porous structure generated from anion exchange. High specific surface area prompted a high degree of exposure of the active sites and made active sites contact with substrates sufficiently. Meanwhile, the fast mass transport in hierarchical pores may also have positive effects on enhancing the catalytic activity.

In order to further demonstrate the positive correlation between catalytic activities of PILs and their specific surfaces area, the N-heterocyclic carbomethoxylation reactions<sup>20</sup> catalyzed by AE-PIL-Cl and DS-PIL-Cl in the presence of dimethyl carbonate (DMC) were investigated (Fig. 5). When using indole as substrate, AE-PIL-Cl gave higher yields (89%) than that of DS-PIL-Cl (68%). Under identical conditions, pyrrole and carbazole as substrates also gave the similar results. The differences of catalytic activities between high specific area porous PILs and nonporous PILs were greater (8% < 21% < 32%) with the increase of the sizes of substrates (pyrrole < indole < carbazole) (Table S3, ESI<sup>†</sup>). All results revealed that increasing specific surface area of PILs and fabricating hierarchical porous structure by anion exchange can improve the accessibility of reactants to active sites and get more superior catalytic activity.

In summary, we have successfully developed a novel synthetic method to hierarchical porous poly(ionic liquid)s *via* exchanging the salicylate and its dimers/clusters of PILs to other smaller anions. The obtained PILs have structurally stable nanoparticle morphology and hierarchical porous structure with the high specific surface area. Besides, the hierarchical porous PILs show superior catalytic activity in the cycloaddition reactions of CO<sub>2</sub> with epoxides and N-heterocyclic carbomethoxylation reactions. And a positive correlation between catalytic activities of PILs and their specific surface area was obtained. High specific surface area prompted a high degree of exposure of the active sites and the fast mass transport in hierarchical pores improved the accessibility of reactants to active sites, enhancing catalytic

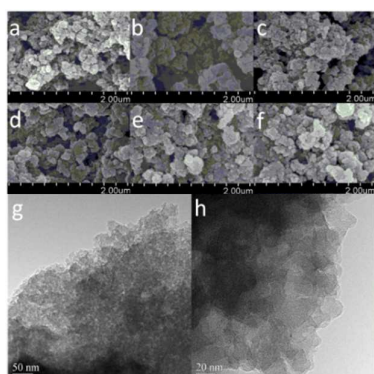


**Fig. 3** SEM images of a) AE-PIL-Cl; b) AE-PIL-Br; c) AE-PIL-OAc; d) DS-PIL-Cl; e) DS-PIL-Br; f) DS-PIL-OAc; TEM images of AE-PIL-Cl g) 50 nm; h) 20 nm.

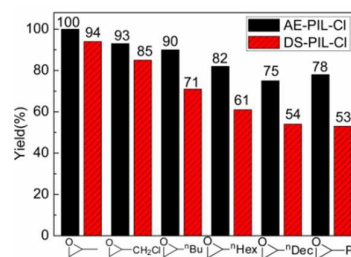


**Fig. 4** The activity of AE-PIL-Cl and DS-PIL-Cl in cycloaddition reactions of CO<sub>2</sub> and epoxides. Reaction condition: Substrate (5 mmol) CO<sub>2</sub> (1 MPa), catalyst (1 mol% based on imidazolium), 140 °C, 6 h.

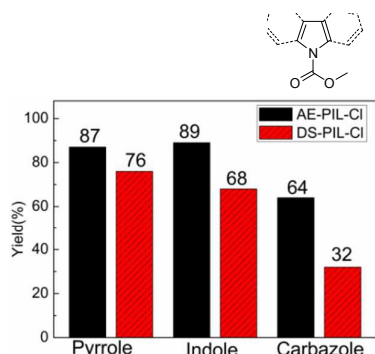


**Fig. 5** The activity of AE-PIL-Cl and DS-PIL-Cl in N-heterocyclic carbomethoxylation reactions. Reaction condition: Substrates (1 mmol), DMC (10 mL), catalyst (10 mol% based on imidazolium), 110 °C, 9 h.

activity.

The authors are grateful to financial support from the National Natural Science Foundation of China (Grant No. 21573072) and Shanghai Leading Academic Discipline Project (Grant No. B409).

## Notes and references

- (a) J. Yuan, D. Mecerreyes and M. Antonietti, *Prog. Polym. Sci.*, 2013, **38**, 1009–1036; (b) D. Mecerreyes, *Prog. Polym. Sci.*, 2011, **36**, 1629–1648; (c) J. Yuan and M. Antonietti, *Polymer*, 2011, **52**, 1469–1482; (d) J. Lu, F. Yan and J. Texter, *Prog. Polym. Sci.*, 2009, **34**, 431–448; (e) M. D. Green and T. E. Long, *Polym. Rev.*, 2009, **49**, 291–314.
- (a) Y. Zhang, B. Wang, E. H. M. Elageed, L. Qin, B. Ni, X. Liu, and G. Gao, *ACS Macro Lett.*, 2016, **5**, 435–438; (b) Q. Wang, Y. Geng, X. Lu and S. Zhang, *ACS Sustainable Chem. Eng.*, 2015, **3**, 340–348; (c) X. Kang, J. Zhang, W. Shang, T. Wu, P. Zhang and B. Han, *J. Am. Chem. Soc.*, 2014, **136**, 3768–3771; (d) T. Shi, J. Wang, J. Sun, Mi. Wang, W. Cheng and S. Zhang, *RSC Adv.*, 2013, **3**, 3726–3732.
- (a) P. Wang, Y. Zhou, J. Luo and Z. Luo, *Polym. Chem.*, 2014, **5**, 882–891; (b) B. N. Reddy and M. Deepa, *Polymer*, 2013, **54**, 5801–5811; (c) J. Yuan, A. G. Marquez, J. Reinacher, C. Giordano, J. Janek and M. Antonietti, *Polym. Chem.*, 2011, **2**, 1654–1657.
- (a) M. D. R. Nabid, Y. Bide and Z. Habibi, *RSC Adv.*, 2015, **5**, 2258–2265; (b) Y. Ye, H. Wang, S. Bi, Y. Xue, Z. Xue, Y. Liao, X. Zhou, X. Xie and Y. Mai, *Carbon*, 2015, **86**, 86–97; (c) C. Liao, R. Liu, X. Hou, X. Sun and S. Dai, *New Carbon Mater.*, 2014, **29**(1), 78–80.
- (a) A. Okafuji, Y. Kohno and H. Ohno, *Macro. Rapid Comm.*, 2016, **34**(14), 1130–1134; (b) B. Ziolkowski and D. Diamond, *Chem. Commun.*, 2013, **49**, 10308–10310.
- (a) M. G. Cowan, D. L. Gin and R. D. Noble, *Acc. Chem. Res.*, 2016, **49**, 724–732; (b) J. Gong, H. Lin, M. Antonietti and J. Yuan, *J. Mater. Chem. A*, 2016, **4**, 7313–7321; (c) J. E. Bara, D. L. Gin and R. D. Noble, *Ind. Eng. Chem. Res.*, 2008, **47**, 9919–9924; (d) J. E. Bara, S. Lessmann, C. J. Gabriel, E. S. Hatakeyama, R. D. Noble and D. L. Gin, *Ind. Eng. Chem. Res.*, 2007, **46**, 5397–5404.
- Z. Wu, C. Chen, Q. Guo, B. Li, Y. Que, L. Wang, H. Wan and G. Guan, *Fuel*, 2016, **184**, 128–135.
- C. Gao, G. Chen, X. Wang, J. Li, Y. Zhou and J. Wang, *Chem. Commun.*, 2015, **51**, 4969–4972.
- X. Wang, Y. Zhou, Z. Guo, G. Chen, J. Li, Y. Shi, Y. Liu and J. Wang, *Chem. Sci.*, 2015, **6**(12), 6916–6924.
- A. Dani, Elena. Groppo, C. Barolo, J. G. Vitillo and S. Bordiga, *J. Mater. Chem. A*, 2015, **3**, 8508–8518.
- S. Soll, P. Zhao, Q. Zhao, Y. Wang and J. Yuan, *Polym. Chem.*, 2013, **4**, 5048–5051.
- F. Liu, L. Wang, Q. Sun, L. Zhu, X. Meng and F. S. Xiao, *J. Am. Chem. Soc.*, 2012, **134**, 16948–16950.
- (a) A. Wilke, J. Yuan, M. Antonietti and J. Weber, *ACS Macro Lett.*, 2012, **1**, 1028–1031; (b) J. Huang, C. Tao, Q. An, W. Zhang, Y. Wu, X. Li, D. Shen and G. Li, *Chem. Commun.*, 2010, **46**, 967–969.
- (a) K. Täuber, B. Lepenies and J. Yuan, *Polym. Chem.*, 2015, **6**, 4855–4858; (b) K. Täuber, A. Zimathies and J. Yuan, *Macromol. Rapid Commun.*, 2015, **36**, 2176–2180; (c) Q. Zhao, J. Heyda, J. Dzubiella, K. Täuber, J. W. C. Dunlop and J. Yuan, *Adv. Mater.*, 2015, **27**, 2913–2917; (d) Z. Zhang, Q. Zhao, J. Yuan, M. Antonietti and F. Huang, *Chem. Commun.*, 2014, **50**, 2595–2597; (e) K. Zhang, X. Feng, X. Sui, M. A. Hempenius and G. J. Vancso, *Angew. Chem. Int. Ed.*, 2014, **53**, 13789–13793; (f) Q. Zhao, M. Yin, A. Zhang, S. Prescher, M. Antonietti and J. Yuan, *J. Am. Chem. Soc.*, 2013, **135**, 5549–5552; (g) Q. Zhao, S. Soll, M. Antonietti and J. Yuan, *Polym. Chem.*, 2013, **4**, 2432–2435.
- (a) A. Itxaso, G. Ignacio, C. P. M., G. Aratz, T. Marek, J. Manfred, W. Krzysztof, C. German and I. Odriozola, *ChemsusChem.*, 2014, **7**, 3407–3412; (b) X. Feng, C. Gao, Z. Guo, Y. Zhou and J. Wang, *RSC Adv.*, 2014, **4**, 23389–23395; (c) S. Soll, Q. Zhao, J. Weber and J. J. Yuan, *Chem. Mater.*, 2013, **25**, 3003–3010.
- (a) M. Dule, M. Biswas, T. K. Paira and T. K. Mandal, *Polymer*, 2015, **77**, 32–41; (b) L. Han, H. J. Choi, D. K. Kim, S. W. Park, B. Liu and D. W. Park, *J. Mol. Catal. A: Chem.*, 2011, **338**, 58–64; (c) D. Katsigiannopoulos, E. Grana, A. Avgeropoulos, P. M. Carrasco, I. Garcia, I. Odriozola, E. Diamanti and D. Gournis, *J. Polym. Sci. Pol. Chem.*, 2012, **50**, 1181–1186.
- (a) J. Gujt, Č. Podlipnik, M. Bešterrogač and E. Spohr, *Phys. Chem. Chem. Phys.*, 2014, **16**, 19314–19326; (b) S. K. Das, M. K. Bhunia, M. S. Motin, S. Dutta and A. Bhaumik, *Dalton Trans.*, 2011, **40**, 2932–2939; (c) B. Greener, S. J. Archibald and M. Hodgkinson, *Angew. Chem. Int. Ed.*, 2000, **39**, 3601–3603.
- (a) M. F. Rojas, F. L. Bernard, A. Aquino, J. Borges, F. D. Vecchia, S. Menezes, R. Ligabue and S. Einloft, *J. Mol. Catal. A: Chem.*, 2014, **392**, 83–88; (b) S. G. Esfahani, H. Song, E. Păunescu, F. D. Bobbink, H. Liu, Z. Fei, G. Laurenczy, M. Bagherzadeh, N. Yan and P. J. Dyson, *Green Chem.*, 2013, **15**, 1584–1589; (c) S. Wu, B. Wang, Y. Zhang, E. H. M. Elageed, H. Wu and G. Gao, *J. Mol. Catal. A: Chem.*, 2016, **418**, 1–8.
- A. L. Girard, N. Simon, M. Zanatta, S. Marmitt, P. Gonçalves and J. Dupont, *Green Chem.*, 2014, **16**, 2815–2825.
- X. Fu, Z. Zhang, C. Li, L. B. Wang, H. Ji, Y. Yang, T. Zou and G. Gao, *Catal. Commun.*, 2009, **10**, 665–668.